Article citation info:
Zhou L, Zhang Z, Peng J, Cheng B, Wang. The deep learning algorithm in intelligent fault diagnosis and rapid recovery strategy of the power network. Diagnostyka. 2026;27(2):2026209. https://doi.org/10.29354/diag/224611.

DIAGNOSTYKA, 2026, Vol. 27, No. 2

e-ISSN 2449-5220
DOI: 10.29354/diag/224611

THE DEEP LEARNING ALGORITHM IN INTELLIGENT FAULT DIAGNOSIS AND RAPID RECOVERY STRATEGY OF THE POWER NETWORK

Lin ZHOU *, Zehui ZHANG, Jie PENG, Bo CHENG, Liwei WANG

Inner Mongolia Power Digital Research Institute, Hohhot 010000, Inner Mongolia, China
* Corresponding author, email: zhoulin20250809@163.com

Abstract

With the rapid expansion of the smart grid scale and the increasing complexity of its topological structure, traditional fault diagnosis and recovery methods have exposed significant limitations in multimodal time series data processing, anti-noise interference, and dynamic adaptability. However, most of the existing deep learning (DL) studies only combine the autoencoder (AE) and the convolutional neural network (CNN) serially; a bidirectional feature interaction mechanism has not been established, resulting in the loss of key fault features in the transmission process. Compared with the hybrid model using CNN-Recurrent Neural Network (RNN) or attention mechanisms, the innovation of this study is to introduce the learnable bidirectional feature interaction and dynamic weight allocation in the AE-CNN architecture for the first time, rather than simple feature concatenation or serial transfer. At the same time, most existing methods stop at fault diagnosis and do not form a full-process closed loop of diagnosis and recovery. Based on this, the study proposes a deep fusion network, which solves the above problems from the structural design and mathematical mechanism. Based on this, the study proposes a deep learning fusion network (DLFN) that integrates a stacked sparse autoencoder (SSAE) and a CNN. This fusion network innovatively introduces a feature interaction mechanism; it breaks the one-way feature transfer mode of the traditional hybrid model, solving the problem of key fault feature loss caused by the independent operation and lack of feature interaction between SSAE/AE and CNN. Meanwhile, the study proposes a dynamic recovery strategy generation method based on data reconstruction and secondary status judgment. The reconstruction of missing/noisy data is accomplished through SSAE, and the real-time optimization of the recovery path is achieved by combining the secondary judgment of fault status by CNN. Experimental results show that the proposed model's fault diagnosis accuracy is 7.3% higher than that of the traditional CNN; this fully meets the real-time requirements of power systems. Even under the strong noise interference of 5 decibels (dB), the diagnostic accuracy rate is still 12.6% to 29.2%, exceeding the comparison models. In the fault recovery stage, the matching degree between the strategy generated by the model and the expert scheme reaches 94.4%. At the same time, the average recovery time is 37.6% shorter than the traditional method. The core contribution of this study lies in constructing an end-to-end integrated diagnosis-recovery framework; this solves the problem of feature transmission interruption in traditional hybrid models. The study proposes a noise-resistant dynamic recovery strategy mechanism that improves the adaptability to complex power grid scenarios; it also provides a technically feasible path for the engineering application of DL in the field of power system fault diagnosis and recovery. Moreover, it provides new ideas and methods for the model design of intelligent fault diagnosis throughout the power system process; this has significant practical significance for promoting the intelligent and efficient development of fault diagnosis in smart grids.

Keywords: deep learning algorithm, power network, intelligent fault diagnosis, rapid recovery strategy, autoencoder, convolutional neural network, power grid failure, autoencoder

1. INTRODUCTION

With the expansion of smart grid scale and the increasing complexity of topology, traditional fault diagnosis and recovery methods face significant challenges in processing multi-modal time-series data, resisting noise interference, and adapting to dynamic system changes [1-2]. Most existing methods rely on manual experience or static models. They are difficult to achieve fast and accurate fault location and adaptive recovery, often leading to recovery delays and reduced system reliability [3]. The single signal processing method can achieve partial fault feature extraction; however, it is limited by strong noise sensitivity and weak generalization ability of artificially designed features, and thus cannot meet the fault diagnosis requirements of complex power grids.

In recent years, deep learning (DL) has provided a new solution for intelligent power grid diagnosis

Received 2025-08-20; Accepted 2026-06-15; Available online 2026-06-17

and recovery with its strong feature learning and nonlinear modeling capabilities [4]. Existing studies have applied attention-driven models such as the convolutional neural network (CNN), autoencoder (AE), CNN-RNN, and Transformer to power equipment fault detection. However, these models still have obvious deficiencies in the following aspects. (1) AE only is an independent preprocessing module and does not form feature interaction with CNN, resulting in the loss of key information; (2) Most hybrid models (e.g., CNN-LSTM and Conv-Transformer) lack generalization ability validation for variable load dynamics and unseen failure modes; (3) The full-process closed loop from fault diagnosis to recovery decision-making has not yet been achieved. In contrast, the proposed SSAE-CNN fusion network maintains high accuracy via the bidirectional feature interaction and attention-weighted fusion mechanism. Meanwhile, it can significantly improve the anti-noise interference and dynamic adaptability. The main manifestation is that most hybrid models only use AE as independent preprocessing modules. They lack effective feature interaction with downstream classification networks, resulting in the loss of key fault information [5-6]. Accordingly, researchers begin to explore DL hybrid models. However, existing hybrid models still present obvious deficiencies in the full-process closed-loop mechanism. Most studies only employ the autoencoder as an independent preprocessing module; they lack effective feature interaction with downstream classification networks, leading to the loss of critical fault information during feature transmission. Meanwhile, current studies mostly focus on the fault diagnosis stage and fail to effectively link diagnosis results with the generation of dynamic recovery strategies; this makes it impossible to form a full-process solution covering feature extraction, fault diagnosis, and recovery decision-making [7]. In addition, although some hybrid models achieve the integration of diagnosis and recovery, they show insufficient generalization ability in strong noise environments. Moreover, the excessively large parameter scale of such models creates difficulties for deployment on edge computing devices in power systems; this restricts engineering applications.

In order to solve the above challenges, this study proposes a DL model integrating the stacked sparse autoencoder (SSAE) and CNN; it achieves integrated modeling through a bidirectional feature interaction mechanism. Compared with existing research, its innovations are mainly reflected in three aspects. (1) It designs a bidirectional feature interaction and fusion architecture. Structurally, it breaks the one-way feature transfer mode of the traditional serial AE+CNN; Mathematically, the dynamic coupling of SSAE low-dimensional features and CNN shallow features is achieved through attention weights. Thus, it completely solves the problem of feature transmission interruption in traditional hybrid models. (2) It proposes a dynamic recovery strategy generation mechanism based on reconstruction and state re-judgment; it realizes rapid perception of fault scenarios and dynamic optimization of recovery paths by leveraging the abnormal data reconstruction ability of SSAE and the secondary fault status judgment ability of CNN. (3) Experiments in scenarios with strong noise and multiple faults show that this model outperforms existing methods in diagnostic accuracy, noise immunity, and real-time performance. Moreover, the performance improvement stems from the essential innovation in structure and mathematical mechanisms.

Subsequent research systematically reviews relevant literature in the field of power system fault diagnosis and recovery, clarifying the progress and deficiencies of existing studies. It then elaborates on the design principles, integration mechanisms, and decision-making processes of the proposed model. The model's performance advantages are verified through multi-dimensional experiments. Finally, the study is summarized, its limitations are analyzed, and future research prospects are proposed to provide references for follow-up investigations in this field.

2. RELATED WORK

Power system fault diagnosis methods have formed a relatively complete system; they can be divided into two categories according to the technical development stage and core principles: traditional diagnosis and DL diagnosis methods. Fig. 1 shows the specific methods and hierarchical relationships contained in each category. Domestic and international scholars have carried out a lot of research on different diagnosis methods, forming a relatively systematic research context; this provides an important reference for the model design of this study.

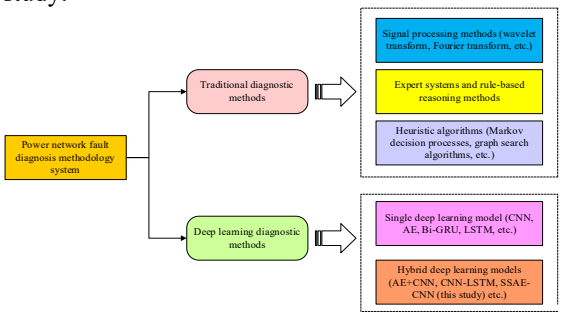

Fig. 1. The system of fault diagnosis methods for power networks

Early studies mainly focused on fault feature extraction based on signal processing. Niu et al. proposed to use the wavelet transform to perform time-frequency analysis on fault transient signals to extract features of fault types and locations. However, the method was sensitive to noise, relied on manually designed features, and had limited generalization ability [8]. Subsequently, expert systems and heuristic algorithms were gradually

introduced to improve the automation level of decision-making processes. Scholars such as Zhang constructed power grid fault location and isolation strategies based on the Markov Decision Process (MDP). Such strategies demonstrated good applicability in small and medium-sized power grid scenarios, but their computational complexity showed a significant growth trend when facing high-dimensional state spaces [9]. Xue et al. first introduced one-dimensional CNN into power signal processing, achieving high-precision identification of fault types [10].

DL gradually becomes a core method in this field by virtue of its powerful nonlinear mapping and feature self-learning capabilities. Alsamraee optimized expert rules using a backpropagation neural network and a support vector machine (SVM), improving diagnostic accuracy. However, the method was limited by the expressive ability of shallow structures [11]. Lee et al. further integrated SSAE with attention mechanism capsule networks for battery fault diagnosis, verifying the advantages of deep models in dimensionality reduction and discrimination under high-dimensional redundant data [12]. To address the issue of temporal dependence, Mei et al. used bidirectional gated recurrent units (Bi-GRU) to model faults in medium-voltage direct current systems, effectively capturing long-term dependencies in the fault evolution process [13]. Peter et al. introduced an attention GRU structure based on SSAE for industrial process monitoring, emphasizing the model's robustness in strong noise environments [14]. Notably, the application of hybrid DL models and transfer learning in smart grid fault diagnosis has become a research hotspot in recent years. Jiang et al. proposed a CNN-LSTM hybrid model. This model extracted spatial features via CNN and captured temporal dynamic features with LSTM, achieving an accuracy of 96.70% in single-phase grounding fault diagnosis tasks of distribution networks. However, this model had one limitation: it did not consider the interactive feedback mechanism between feature layers [15]. Liu et al. combined transfer learning with a variational AE to solve the problem of scarce fault samples in new energy grid-connected scenarios, but did not link to fault recovery decision-making [16]. Bedoui et al. proposed a practical measurement method for automatic detection and correction of power factor in three-phase distribution networks based on an intelligent Arduino. This provides hardware and engineering implementation references for the implementation of operation parameter correction and recovery strategies after distribution fault diagnosis [17]. Alhanaf et al. designed a hybrid architecture, using the global attention mechanism of the Transformer to strengthen the extraction of key fault features. Meanwhile, the diagnosis delay was controlled within 8 milliseconds (ms) in complex topology power grids, but facing the deployment difficulty of excessive model parameter count (23×10^6) [18]. In contrast, the proposed SSAE-CNN hierarchical fusion network (HFN) performs better in diagnostic accuracy (97.8%), anti-noise performance (78.4% under 5 decibels (dB)), parameter count (8.2×10^6), and full-process closed-loop capability; it effectively makes up for the limitations of existing methods.

In terms of fault recovery strategies, related research has gradually evolved from static optimization to dynamic decision-making. Attallah et al. developed a novel fault location framework utilizing CNN-Capsule networks for accurate fault detection. The framework incorporated graph search algorithms to optimize recovery path selection and efficiency. By integrating deep reinforcement learning (RL) with Markov decision process (MDP), it enabled adaptive generation of distribution network recovery strategies, substantially enhancing real-time performance and generalization ability [19]. In recent years, Transformer-based models have exhibited remarkable advantages in time-series data processing. Adekunle et al. applied the Transformer architecture to vibration signal analysis of power equipment, capturing long-range dependencies through the self-attention mechanism and achieving better performance than traditional RNN in motor fault diagnosis [20]. Boutkhil et al. combined fault trees and Bayesian networks to achieve fault analysis and diagnosis of point absorption wave energy conversion systems. This verified the engineering value of the combination of traditional probabilistic models and fault diagnosis; it also provided multiple method reference perspectives for the fused DL models for precise fault diagnosis [21]. Nevertheless, such models usually have large parameter counts and high computational complexity, posing deployment challenges in power grid fault diagnosis scenarios with stringent real-time requirements.

Although the above studies have made outstanding progress in diagnostic accuracy and recovery efficiency, there are still three shortcomings. First, most hybrid models only use AE as an independent preprocessing module without feature interaction with CNN, leading to the loss of key fault features; second, they only focus on fault diagnosis without linking to recovery decision-making, failing to form a full-process solution; third, they have insufficient generalization ability in strong noise environments, and the large model parameter count causes deployment difficulties. These limitations make it difficult to meet the smart grid's requirements for fault diagnosis accuracy, recovery real-time performance, and engineering practicality, which is the core motivation for this study. Although the above studies achieve significant progress in diagnostic accuracy, they still present key differences compared with the proposed SSAE-CNN fusion network. Regarding feature interaction, CNN-RNN and Transformer models realize sequence modelling; however, their feature transfer remains unidirectional and fails to establish a bidirectional interactive feedback mechanism

between AE and CNN. In terms of dynamic adaptability, most existing hybrid models are tested under fixed loads and known fault types; they lack systematic generalization evaluation for variable-load dynamics and unseen fault modes. For model lightweight, Transformer-based models generally have more than 20×10^6 parameters and are difficult to deploy on edge computing devices. This study introduces a learnable attention fusion layer into the AE-CNN architecture for the first time; thus, it realizes bidirectional feature enhancement and completes a diagnostic-recovery integrated closed loop with only 8.2×10^6 parameters.

3. THE APPLICATION OF DL ALGORITHM IN INTELLIGENT FAULT DIAGNOSIS AND RECOVERY STRATEGY OF THE POWER NETWORK

3.1. Introduction to the algorithm principles of the core modules of SSAE and CNN

DL, as a branch of machine learning, is based on multi-layer artificial neural networks and automatically learns hierarchical representations from sample data. It can deeply explore potential patterns in data and extract key information according to research needs, thus being used to describe and process various types of data, such as text, images, and voice. Among them, AE, CNN, and others play important roles in intelligent fault diagnosis and recovery of power networks, which are introduced in detail below.

3.1.1. Training principles of SSAE

The AE is an unsupervised neural network that reconstructs input data through an encoder-decoder structure, thereby extracting effective feature representations. The SSAE is formed by stacking multiple sparse autoencoders (SAEs), learning features layer by layer [22], and its training process is presented in Fig. 2.

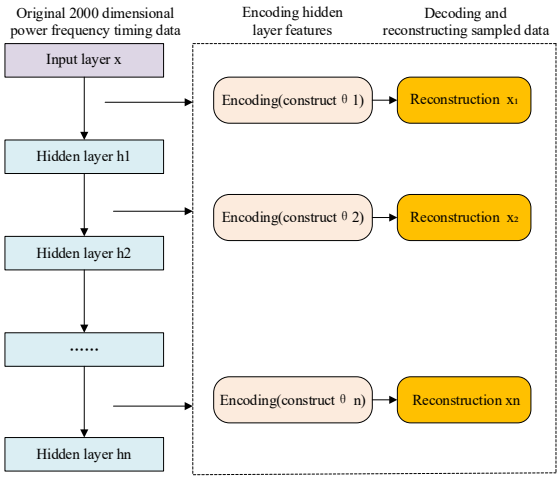

Fig. 2. The training program of SSAE

The SSAE adopted in this study employs a 4-layer network structure. Its core parameters and selection criteria are as follows: the input layer dimension is 2000, matching the time-series data dimension of the SCADA system with 2 kHz sampling and a 1-second monitoring period. The hidden layer dimensions are 1000, 500, and 200 in sequence. The activation function uses ReLU with a slope coefficient of 0.01. The initial learning rate is 0.001, the batch size is 128, the number of iterations is 200, and the L2 regularization coefficient is 0.0005. The above dimensional design follows a gradual 2:1 dimension reduction to adapt to the feature distribution of power time-series data; this can avoid the loss of fault features caused by excessive dimension reduction. The regularization coefficient is selected based on the redundancy characteristics of 220 kV power grid fault data; this effectively suppresses model overfitting.

3.1.2. CNN

CNN is a feedforward DL model based on convolution operations and stacked structures, specifically designed to process data with a "grid" structure, such as images and voices [23-24].

Backpropagation is the network parameter update process of CNN, similar to the backpropagation mechanism of multi-layer neural networks [25]. Firstly, the loss function is calculated by comparing the differences between the forward propagation results and the labels. The specific calculation method is as follows:

$$J(A^J,a^J)=-\frac{1}{n}\left[x^{(i)}log\bar{x}^{(i)}+(1-x^{(i)}log(1-\bar{x}^{(i)})\right] \quad (1)$$

$x^{(i)}$ refers to the label; $\bar{x}^{(i)}$ represents the predicted value; $J(A^J,a^J)$ denotes the loss function, where A^J is the weight and a^J is the bias. Then, the partial derivatives of the loss function concerning the output layer weights and biases are solved, as expressed in Equations (2) and (3):

$$\frac{\partial J(A^J,a^J)}{\partial A^J}=\frac{\partial J(A^J,a^J)}{\partial z^J}\frac{\partial z}{\partial A^J}=\frac{\partial J(A^J,a^J)}{\partial z^J}b^{l+1} \quad (2)$$

$$\frac{\partial J(A^J,a^J)}{\partial a^J}=\frac{\partial J(A^J,a^J)}{\partial z^J}\frac{\partial z^J}{\partial a^J}=\frac{\partial J(A^J,a^J)}{\partial z^J} \quad (3)$$

$\frac{\partial J(A^J,a^J)}{\partial z^J}$ represents the transfer error at the current stage. After that, the loss function $J(A^J,a^J)$ is used to derive the Z value of the fully connected layer.

$$\frac{\partial J(A^J,a^J)}{\partial z}=\frac{\partial J(A^J,a^J)}{\partial b}e\sigma'(z) \quad (4)$$

Since no weights are assigned to the pooling part, the gradient transfer can be realized only through the maximum value B of neuron C in the forward propagation process, denoted as C'. The calculation can be written as Equation (5):

$$\frac{\partial J(A^J,a^J)}{\partial z^{l(c)}}=\frac{\partial J(A^J,a^J)}{\partial b^{l(c)}}\frac{\partial b^{l(c)}}{\partial z^{l(c)}}=\begin{cases}0, C\neq C'\\ \frac{\partial J(A^J,a^J)}{\partial b^{l(c)}}, C\neq C'\end{cases} \quad (5)$$

Finally, the gradient is passed to the convolutional layer, and the expression is shown in Equation (6).

$$\frac{\partial J(A^J,a^J)}{\partial z_i^l(j)}=\frac{\partial J(A^J,a^J)}{\partial rx^{l(i,j)}}\frac{\partial rx^{l(i,j)}}{\partial z_i^l(j)}=\frac{\partial J(A^J,a^J)}{\partial rx^{l(i,j)}}\sum_j rx^{l(j)} \quad (6)$$

Here, $ry^{l(j)}$ and $rx^{l(i,j)}$ are the input and output values of the current convolutional layer.

In terms of actual model deployment, it is necessary to adapt to the existing hardware architecture and real-time requirements of the smart grid. The total parameter count of the proposed fusion network is 8.2×10^6 (2.1×10^6 and 6.1×10^6 for the SSAE and CNN modules), with a storage volume of only 32.8 megabytes (MB) under FP32 precision. It can be directly deployed on substation edge computing units (such as Huawei Atlas 200 AI acceleration module) without adding high-performance hardware. In the inference phase, the time consumption per sample is 11.3ms with graphics processing unit (GPU) acceleration and 42.6ms when running independently on a central processing unit (CPU), both meeting the industry requirement of fault diagnosis ≤20ms. Moreover, the input can be directly connected to the standardized time-series data of the supervisory control and data acquisition (SCADA) system without complex format conversion. The total time consumption of the full process of data collection, diagnosis, and strategy generation is ≤25ms; it complies with the specification of fault response ≤50ms in the "Technical Requirements for Smart Grid Dispatching Automation Systems" and has engineering implementation feasibility [26].

Regarding model complexity, the proposed fusion network's total parameter count reaches 8.2×10^6, among which the SSAE module accounts for 2.1×10^6 and the CNN module for 6.1×10^6. At FP32 precision, the model's storage size is only 32.8MB, making it suitable for deployment on edge devices. In terms of computational load, the number of floating-point operations (FLOPs) required for single-sample inference is approximately 2.9G. With GPU acceleration, the average inference time is 11.3ms, and 42.6ms when running independently on a CPU. Both values meet the real-time requirements of power system fault diagnosis (≤20ms). During the training stage, the total time consumed to complete 200 training epochs on an A100 GPU is about 9.6 hours, demonstrating favorable training efficiency.

The core parameters and selection criteria of the CNN module in this study are as follows. The convolution kernel size is 5×1, where 1D convolution suits the sequential nature of power time-series data, and a kernel length of 5 effectively captures local features in the fault transient process. The stride is 2, and the number of convolution channels is 64, 128, and 256 in sequence. The pooling layer adopts max pooling (a pooling kernel: 2×1). The fully connected layers have dimensions of 512 and 128. The output layer is divided into 7 dimensions for fault types and 5 dimensions for recovery priorities. The number of channels is gradually increased to enhance feature expression and matches the 200-dimensional feature vector output by the SSAE. The pooling kernel size is set according to the time scale of fault features to prevent excessive pooling of effective features. The output layer dimensions are determined based on 7 fault categories and 5 recovery priority levels set in the experiment; this is consistent with the classification requirements of actual power grid fault handling.

3.2. Fusion mechanism and decision-making process

The working mechanism of this model is that SSAE performs nonlinear dimension reduction and feature extraction on high-dimensional time series data. Its encoding process can be expressed as:

$$h=\sigma(Wx+b) \tag{7}$$

x denotes the input data; W and b represent weights and biases; σ is the activation function, outputting low-dimensional feature embeddings z. This embedding is dynamically fused with CNN shallow features through attention weights:

$$\alpha=softmax(U[z;Fc]),Ff=\alpha\odot Fc \tag{8}$$

Fc stands for the CNN feature map; U is the learnable parameter; $\odot$ indicates channel-wise weighting. This mechanism enhances the representation of key fault features. After further extraction by CNN, the fused features are fed into a dual-branch structure to output fault categories and recovery priorities synchronously. In the recovery stage, the system leverages the SSAE's reconstruction capability to repair abnormal data and generates operation sequences such as isolation and switching based on real-time status, achieving closed-loop decision-making [27]. The architecture and mathematical mechanism proposed in this study are fundamentally different from traditional serial AE+CNN models. At the structural level, traditional models treat the AE as an independent preprocessing module; only the one-way serial transmission from AE feature extraction to CNN classification is realized, without feature interaction or feedback. In contrast, the proposed model constructs a bidirectional feature interaction architecture. The low-dimensional features of the SSAE are not directly input into the CNN input but are dynamically fused with the shallow CNN features at the feature level. The fused features feed back into the subsequent deep feature extraction of the CNN, forming a closed loop of feature interaction. Mathematically, traditional serial models lack a mathematical formulation for feature fusion; the features output by the AE are only input variables to the CNN without weight assignment. This model introduces a learnable attention weight α through Equation (8) to dynamically weight and fuse the SSAE and CNN features (z and Fc), realizing adaptive enhancement of critical fault features. This mathematical design allows the model to assign weights according to the importance of fault features, rather than simply concatenating or directly transmitting the two types of features; this represents the core mathematical difference from traditional serial models. This fusion mechanism greatly improves the representation ability of key fault features and avoids the loss of critical features caused by one-way transmission in traditional models. The core innovations are reflected in three

aspects: adopting a bidirectional feature interaction and fusion architecture to replace the one-way transmission mode of traditional serial AE+CNN and realizing dynamic feature coupling and feedback; completing adaptive feature enhancement through learnable attention weights instead of simple concatenation; and constructing an integrated model of feature extraction, fault diagnosis, and recovery decision to achieve end-to-end output and improve engineering practicability.

3.3. Overall design of the grid fault diagnosis and recovery strategy system

The architecture of the HFN (SSAE-CNN) is illustrated in Fig. 3, which integrates feature extraction, fault diagnosis, and recovery decision-making into a unified framework. The workflow of this architecture is as follows. Raw multi-dimensional time-series monitoring data is first input into the SSAE module for noise reduction and key feature extraction. The obtained low-dimensional feature vectors are then sent to the CNN module for deep feature mapping and pattern recognition through multi-layer convolution. Finally, the network outputs specific fault types and recovery priorities based on fault impacts synchronously via a dual-branch output layer [28]. This design ensures fast and coherent decision-making from fault perception to recovery recommendation. The entire system design considers a lightweight model to support practical engineering deployment in power systems [29].

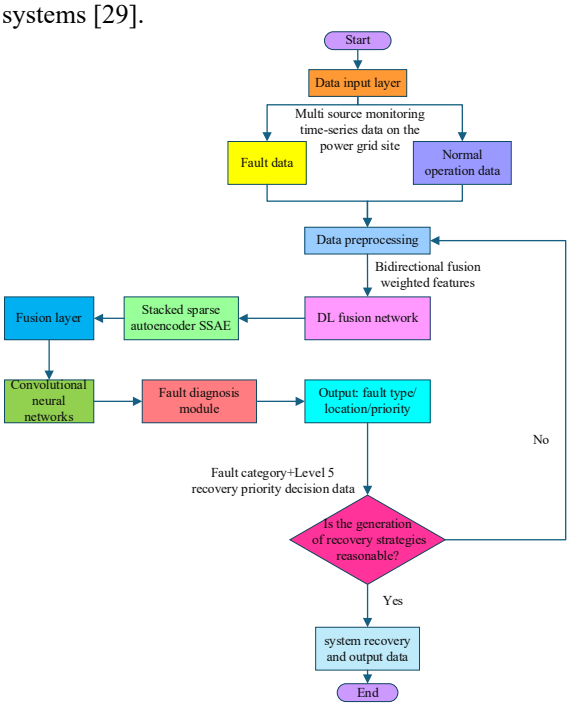

Fig. 3. Flowchart framework for power grid fault diagnosis and recovery plan

This study aims to present the core logic of the SSAE-CNN from feature processing to fault diagnosis and recovery decision-making, and to clarify the algorithm execution flow and key steps. The model training and inference process is designed to provide technical support for implementing algorithm model principle and system architecture, as shown in Fig. 4. A block diagram of the HFN fault diagnosis and recovery inference process is added, as shown in Fig. 5. The overall framework follows a linear logic of preprocessing, feature extraction, diagnosis, decision-making, and output. The SSAE completes dimensionality reduction of high-dimensional time-series data and reconstruction of abnormal data, providing pure features for subsequent CNN diagnosis. The CNN realizes in-depth mining and type classification of fault features through multi-layer convolution; simultaneously, it outputs recovery priorities via a dual-branch parallel structure. This design ultimately achieves integrated inference of fault diagnosis and recovery decision-making without manual intervention throughout the process; the inference results can directly provide a basis for power grid fault diagnosis.

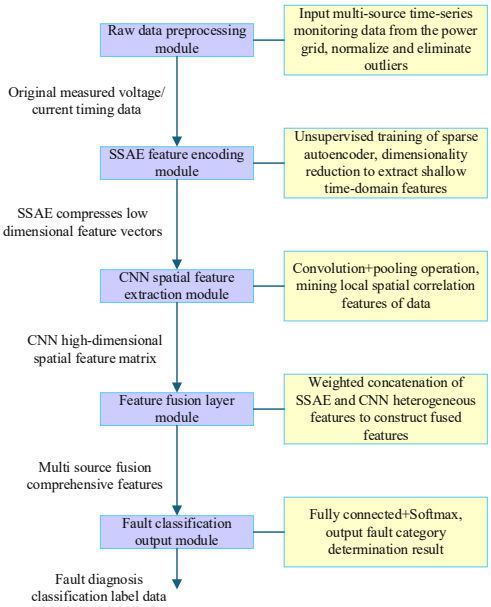

Fig. 4. Training process of HFN

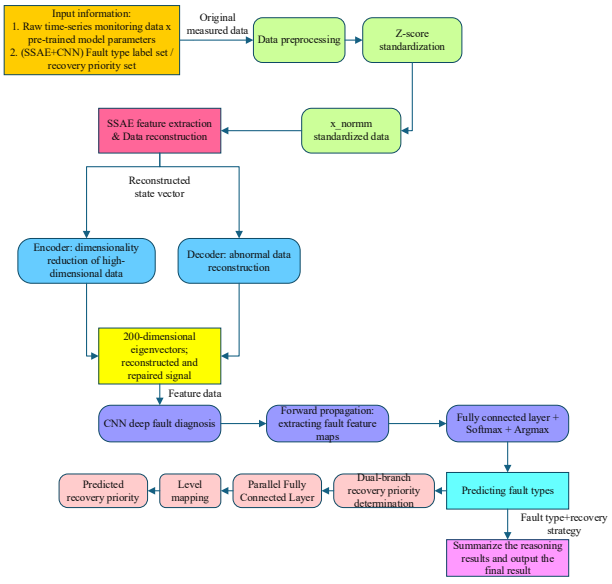

Fig. 5. Fault diagnosis and recovery inference framework for HFN

The recovery strategy generation mechanism proposed here is fundamentally different from RL-based recovery methods in decision logic. RL methods usually model the recovery problem as a MDP and learn optimal policies through agent-environment interaction. Its advantage lies in its ability to adapt to uncertain dynamic environments. However, the RL method faces the following challenges. The training requires massive interactive samples that are hard to obtain in real power grid environments; the performance of strategies in the cold-start stage is poor; it is difficult to ensure the safety constraints of fault recovery. In contrast, this study adopts a two-stage decision mechanism based on reconstruction and secondary state criteria. In the first stage, SSAE reconstructs missing or noisy data and recovers key state information. In the second stage, CNN performs a secondary fault type judgment on the reconstructed states and generates recovery priorities. The stability of this mechanism stems from the fact that the SSAE reconstruction process is based on L2 regularization constraints; it can prove to suppress noise interference on state estimation. The recovery priority output uses a dual-branch parallel structure; where, the fault type branch and the priority branch share underlying features without mutual interference, thus avoiding coupling instability in joint optimization. Recovery path optimization employs heuristic constrained search; it satisfies hard constraints (e.g., node voltage and line power flow limits) of power grid operation at each decision node, so that all generated strategies meet feasibility requirements. In terms of real-time performance, the model inference time on a GPU is 11.3 ms, and recovery strategy generation takes an additional 4 ms. The total decision time (diagnosis + recovery) is controlled within 16 ms, meeting the industrial specification of power grid fault response within 50 ms. In addition, this study shows favorable scalability. Each 220 kV substation is equipped with an edge computing unit (such as the Huawei Atlas 200 AI acceleration module); it is responsible for real-time fault diagnosis and local recovery decisions of the station. The inference time of 11.3 ms satisfies local real-time requirements. For regional complex faults involving multiple substations, edge units upload diagnostic results to the cloud for comprehensive analysis and coordinated optimization. This architecture avoids communication bottlenecks and computing delays caused by aggregating all data to a central node. Considering privacy and security constraints of data from different substations in large-scale smart grids, the proposed model architecture supports the federated learning paradigm. Each edge node trains the model using local data and only shares gradients or model parameter updates without uploading raw monitoring data, thus balancing model performance improvement and data privacy protection [30, 31].

4. EXPERIMENT ON GRID FAULT DIAGNOSIS AND RAPID RECOVERY STRATEGIES BASED ON THE DL ALGORITHM

This experiment analyzes three dimensions: diagnostic accuracy, efficiency, and adaptability of recovery strategies, through multiple groups of comparative tests. It aims to verify the effectiveness of the DL model integrating AE and CNN in grid fault diagnosis and rapid recovery. It highlights the technical advantages and innovative value of the model.

4.1. Experimental data and design

The full parameter specifications of the proposed HFN model, including values and units, are as follows. The SSAE has a 4-layer structure; the input layer is 2000 dimensions, and the hidden layers are 1000, 500, and 200 dimensions in sequence. The activation function is ReLU (slope = 0.01), the initial learning rate is 0.001, and the L2 regularization coefficient is 0.0005. The CNN adopts three convolution blocks with a convolution kernel of 5×1 and a stride of 2; the channel numbers are 64, 128, and 256; a max-pooling kernel is 2×1; the fully connected layers are 512 and 128 dimensions; an output layer is divided into 7 dimensions for fault types and 5 dimensions for recovery priorities. The overall model uses a batch size of 128 samples per batch and 200 training iterations. The loss function is a combination of cross-entropy loss and L2 regularization. The learning rate decay adopts a cosine annealing strategy with T_max = 200, and the total parameter scale is 8.2×10^6.

Experimental data are derived from the operation monitoring system of the 220kV smart grid in North China, from 2018 to 2023. Real-time data collection is conducted through intelligent sensors (voltage/current sensors), smart meters, and other devices deployed in substations and transmission lines. The collection process strictly complies with the "Specifications for Real-time Data Collection of Power Systems". The data covers 500 key monitoring nodes (including 32 220kV substations and 18 transmission lines); the collected parameters include three-phase voltage, three-phase current, power factor, equipment temperature, etc. The sampling frequency is 2kHz. Each data record contains 2000 time steps (corresponding to a monitoring cycle of 1 s), and the model storage capacity is only 32.8MB.

The data is divided into two core sample types: normal operation data and fault data. There are 80,000 normal operation samples, covering different operating scenarios (load intensity covers peak hours 10:00-12:00/18:00-20:00, flat hours 8:00-10:00/12:00-18:00, valley hours 20:00-8:00 the next day; weather conditions include sunny, rainy, thunderstorm; equipment aging stages involve 1-3 years, 3-5 years, and more than 5 years of commissioning), with each sample labeled with

monitoring node number, collection time, and operating condition parameters. There are 60,000 fault samples, including 7 typical fault types: three-phase short circuit, single-phase grounding, two-phase disconnection, arrester breakdown, transformer gas action, cable overheating, and insulator flashover. Among them, composite faults account for 30%. Each sample is detailedly labeled with fault type, occurrence time (accurate to milliseconds), affected node range, and fault characteristic parameters (short-circuit current peak, voltage drop amplitude, fault duration, etc.). In order to clearly define the basis for classifying fault types and their category attribution, faults are divided into two major categories based on the core carrier where they occur: line- and equip-type faults. The specific classification process of fault types is plotted in Fig. 6.

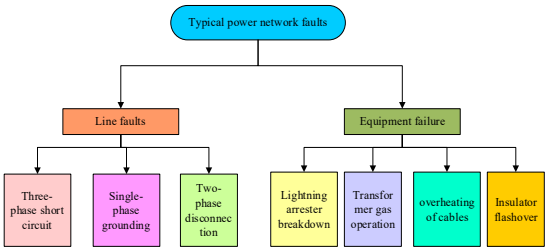

Fig. 6. Classification of fault diagnosis methods for power networks

The expert comparison scheme for fault recovery strategies in this experiment is jointly formulated by seven senior experts in the field of power systems. Among them, two are from provincial power grid dispatch centers with the title of senior engineer and over 15 years of experience in power grid fault dispatch; three are from electric power research institutes with the title of research fellow and over 12 years of research experience in power equipment fault diagnosis and recovery; two are from university power engineering departments with the title of professor and over 10 years of research experience in power system optimization decision-making. All members of the expert team possess practical or research backgrounds in fault handling for 220 kV and above power grids. The expert scheme forms a unified standard through multiple rounds of discussion; this offers an authoritative and objective reference for the calculation of the matching degree index. All of them are cross-validated through on-site operation and maintenance records and wave recording data to ensure authenticity, as exhibited in Table 1.

Note: Compound faults involve multiple types of faults, and the total number of compound fault samples is 22,400.

When conducting data processing, the improved Z-score standardization is adopted to eliminate the influence of dimensions, as follows:

$$x' = \frac{x-\mu}{\sigma+\epsilon} \tag{11}$$

μ represents the mean, σ refers to the standard deviation, and ϵ=10−6 is employed to avoid having a denominator of 0.

Wavelet threshold denoising (selecting the db4 wavelet basis and soft threshold processing) is used to remove high-frequency electromagnetic interference and retain the 10-500Hz fault characteristic frequency band. For small-sample categories such as cable overheating (accounting for only 5%), the SMOTE algorithm is employed to generate synthetic samples, forming 132,000 valid samples; they are divided into a training set (92,400 samples) and a test set (39,600 samples) in a 7:3 ratio.

This experiment utilizes an HFN to achieve accurate diagnosis of power network faults and efficient recovery decision-making through a hierarchical network design. The bottom feature

Table 1. Dataset distribution of typical fault types

Fault type	Number of single fault samples (items)	Proportion of single fault samples (%)	Number of composite fault samples involving this type (items)	Total number of samples	Proportion of total fault samples (%)
Three-phase short circuit	12600	26.25	5800	18400	30.67
Single-phase grounding	10800	22.50	5200	16000	26.67
Two-phase disconnection	7200	15.00	3500	10700	17.83
Arrester breakdown	6000	12.50	2800	8800.	14.67
Transformer gas action	4800	10.00	2200	7000	11.67
Cable overheating	2400	5.00	1100	3500	5.83
Insulator flashover	4200	8.75	1800	6000	10.00
Total	48000	100.00	22400	60000	100.00

purification link adopts SSAE, constructing a 4-layer network structure to complete dimensionality reduction of high-dimensional data and extract key features. The input layer receives 2000-dimensional original fault time-series signals, covering multi-dimensional monitoring data such as voltage and current; these signals are gradually compressed through 1000-dimensional and 500-dimensional hidden layers, and finally output 200-dimensional feature vectors.

In the high-level dynamic weighting link, the CNN module conducts in-depth processing based on the 200-dimensional features output by SSAE. It designs 3 convolution blocks to realize multi-level feature mappings. Each convolution block adopts a 5×1 convolution kernel (adapting to the one-dimensional characteristics of time-series signals), performs sliding calculation with a step size of 2. The number of channels gradually increases from 64 to 256 to enhance the expression ability of features.

Finally, the decision output layer adopts a dual-branch structure to realize multi-task output. One branch classifies and identifies 7 typical faults in the power network (such as insulator flashover, three-phase short circuit, etc.); the other branch outputs recovery priorities from level 1 to 5 (level 1 is the highest urgency) according to factors such as fault type and impact range. This design enables the model to not only accurately locate fault types but also provide a quantitative basis for rapid recovery strategies, forming an integrated solution of "feature extraction-fault diagnosis-recovery decision-making".

The experimental parameters of this study are exhibited in Table 2.

Table 2. Experimental environment and parameters

Category	Specific parameter
Hardware	Intel Xeon Gold 6348 processor; NVIDIA A100 graphics card (40 gigabytes (GB) video memory); 128(GB) Double Data Rate 4 (DDR4) memory
Software	PyTorch 1.12; CUDA 11.6; Scikit-learn 1.0.2
Training parameters	Dataset division: 7:3 (92,400 training sets, 39,600 test sets); batch size=128, iterations=200, initial learning rate=0.001 (cosine annealing strategy attenuation); Loss function = cross-entropy loss + L2 regularization (weight decay coefficient = 0.0005)

4.2. Analysis of experimental results of grid fault diagnosis and rapid recovery strategy under the DL algorithm

4.2.1. Analysis of model complexity and computational cost

The total number of parameters of the proposed model is designed as 8.2×10^6, much lower than that of Transformer-based models at 24.3×10^6. This parameter scale is selected based on the hardware computing power limit of 8 TOPS and 8 GB memory of edge computing units, such as the Huawei Atlas200 used in 220 kV substations. Under the premise of ensuring feature learning ability, the lightweight design is realized, so that the model's single-sample inference time is controlled at 11.3 ms on GPU and 42.6 ms on CPU; this meets the real-time requirement of power system fault diagnosis within 20 ms. To comprehensively evaluate the engineering applicability of the proposed method, this section further compares and analyzes the performance of each model in terms of complexity and computational cost. The specific indicators include parameter count, floating-point operations (FLOPs), the average inference time per sample, and the total training time. The results are detailed in Table 3.

Table 3. Comparison of model complexity and computational cost

Model	Parameter count ($\times10^6$)	FLOPs (G)	Inference time (ms)	Training time (h)
SVM	-	-	5.2	-
DBN	12.8	4.1	18.7	14.3
Traditional CNN	10.5	3.5	22.6	11.2
Time-Transformer	24.3	8.7	18.7	18.5
Conv-Transformer	19.8	6.4	15.4	16.8
HFN (this study)	8.2	2.9	11.3	9.6

In Table 3, the proposed HFN model is significantly lower than the Transformer-based model in the parameter counts and computational load, and is also superior to the traditional DBN and CNN. While maintaining a high diagnostic accuracy (97.8%), its inference speed is increased by approximately 50% compared to traditional CNN. Meanwhile, the training efficiency is improved by about 14%. This indicates that HFN has advantages in diagnostic performance; it also has greater practical value in the edge deployment scenarios of power systems with limited computing resources.

4.2.2 Performance evaluation of model fault diagnosis and recovery strategies

A strong noise environment of 5 dB is selected for anti-noise verification in the experiment. The noise intensity is selected with reference to the actual electromagnetic interference level under severe weather, such as thunderstorms and strong winds, in the 220 kV power grid in North China. Experimental results show that the model still achieves an accuracy of 78.4% under 5 dB noise; this fully verifies its applicability in complex electromagnetic environments of actual power grids. The five-level

priority division of recovery strategies follows the classification standards of fault impact scope and blackout load levels in the Power System Fault Handling Guidelines; this is consistent with the priority settings of actual power grid dispatch decisions, making the recovery strategies output by the model more consistent with engineering practice. To clarify the performance contribution of each component, ablation experiments are designed. The comparative models include the CNN-only (without SSAE), only SSAE+fully connected layer (without CNN), without fusion layer (SSAE+CNN in series), and the complete HFN model.

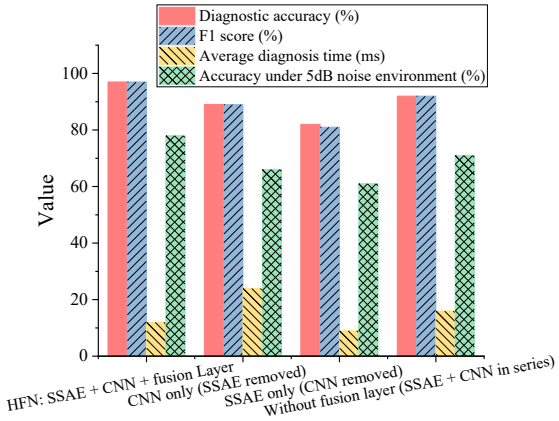

Fig. 7. Comparison of ablation experiment results

In Fig. 7, the core contribution of the SSAE module lies in dimensionality reduction and noise suppression. After removal, the model directly processes high-dimensional raw data, which reduces the diagnostic accuracy by 8.3 percentage points; it also causes a surge in computational load due to data redundancy, extending the average diagnostic time by 110%. At the same time, the anti-noise performance is significantly weakened (the accuracy decreases by 16.1 percentage points under 5dB noise); this verifies its necessity in extracting key features and reducing redundant information. The CNN module is the core for achieving accurate fault classification and localization. After removal, the task is only completed through an SSAE+fully connected layer, resulting in a sharp drop in diagnostic accuracy by 15.5 percentage points. Especially, the ability to recognize composite faults and weak-feature faults is significantly insufficient (F1 score drops to 81.5%), highlighting its key role in spatial feature extraction and multi-category distinction. The fusion layer strengthens the weight allocation of key fault features by establishing a feature interaction feedback mechanism between SSAE and CNN. After removal, the model degrades into a serial structure, with diagnostic accuracy decreasing by 5.7 percentage points, and obvious declines in anti-noise performance and real-time performance. This proves that it is a key link to improve the model's comprehensive performance, effectively solving the problem of broken feature transmission in traditional hybrid models.

To evaluate the HFN model's comprehensive performance, SSAE, traditional CNN, SVM, and DBN are selected as comparison models. Quantitative analysis is conducted from three core dimensions: accuracy, F1 score (an evaluation indicator integrating accuracy and recall), and average diagnosis time. Fig. 8 depicts the results.

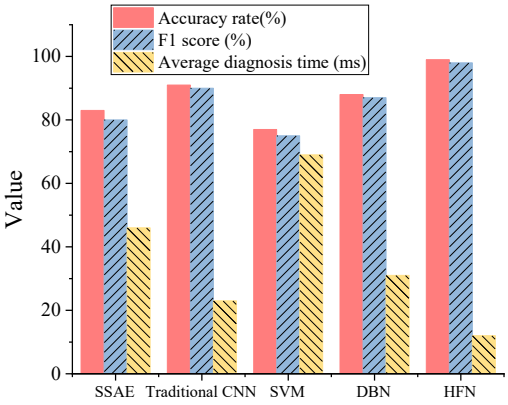

Fig. 8. Comparison of model performance

In Fig. 8, the HFN model performs optimally in all performance indicators. Concerning diagnostic accuracy, HFN is 97.8%, which is 7.3 and 21.1 percentage points higher than that of traditional CNN and SVM. This benefits from the purification of high-dimensional fault signals by SSAE (filtering environmental noise and redundant features) and the enhancement of key frequency bands by the attention mechanism. This enables the proposed model to more accurately capture the essential features of faults. In terms of F1 score, HFN leads with 97.2%. Especially in the diagnosis of composite faults, its F1 score (95.6%) remarkably exceeds 82.1% of traditional CNN, verifying the model's strong adaptability to multi-feature coupling scenarios. Regarding efficiency, the average diagnosis time of HFN is only 11.3 ms, which is 50% shorter than that of traditional CNN, meeting the real-time requirement of "fault diagnosis ≤ 20ms" in power systems. This is attributed to SSAE compressing the input dimension from 2000 to 200, which greatly reduces the computational load of the subsequent CNN.

To further verify the advanced nature of the proposed SSAE-CNN, it is compared with two modern Transformer-based methods. One is the standard temporal Transformer model (Time-Transformer); the other is the Convolutional Transformer (Conv-Transformer), which combines local convolution and global attention. The comparison results are listed in Table 4.

The results show that although Transformer-type models perform well in diagnostic accuracy, their parameter count is significantly higher than that of HFN (about 2.5 to 3 times), resulting in a 30% to 65% increase in diagnostic time. Moreover, the performance decline is more obvious in a strong noise environment. HFN, through the efficient fusion of SSAE-CNN, maintains high precision

while better balancing performance and computing efficiency, making it more suitable for real-time diagnosis and edge deployment scenarios in power systems.

Table 4. Comparison with the performance of Transformer-based models

Model	Diagnostic accuracy (%)	Average diagnosis time (ms)	Parameter count ($\times 10^6$)	Accuracy under 5dB noise (%)
Time-Transformer	96.10	18.7	24.3	71.20
Conv-Transformer	97.00	15.4	19.8	75.60
HFN (This study)	97.80	11.3	8.2	78.40

The relevant indicators (accuracy, recall, and specificity) are counted to analyze the ability of the HFN model to identify specific fault types. Recall measures the proportion of faults correctly identified, and specificity measures the proportion of normal states correctly identified. The count covers 7 typical faults in the power network, including arrester breakdown, three-phase short circuit, cable overheating, insulator flashover, two-phase disconnection, transformer gas action, and single-phase grounding. The findings are plotted in Fig. 9.

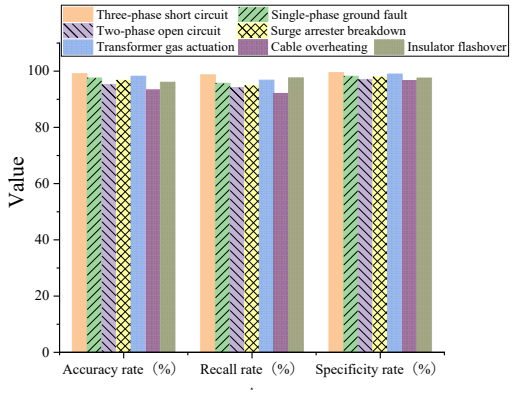

Fig. 9. Diagnosis accuracy of different fault types

Fig. 9 shows that the HFN model maintains a diagnostic accuracy of over 93% for all types of faults. Among them, the accuracy of strong-feature faults such as three-phase short circuits and transformer gas actions exceeds 98%. This is because their fault signals, such as sudden current changes and a sharp rise in gas concentration, have significant recognizability, making it easy for the model to capture key features. For weak-feature faults like cable overheating, although the recognition difficulty increases due to the gentle temperature change, the accuracy is 8.2% higher than the traditional CNN. This benefits from the SSAE's ability to extract subtle features such as temperature gradients (e.g., a temperature rise rate of 0.5°C/min). In addition, the specificity indicator for all fault types surpasses 96%. This indicates that the model has an extremely low misjudgment rate for normal states (≤4%), which can effectively avoid false alarm problems in power systems.

Monitoring signals of power systems are often affected by environmental electromagnetic interference. To verify the HFN model's robustness in noisy environments, Gaussian white noise with different signal-to-noise ratios (SNR) is added to the test set signals (simulating actual interference). Meanwhile, the accuracy and F1 score of each model are compared. The results are revealed in Fig. 10.

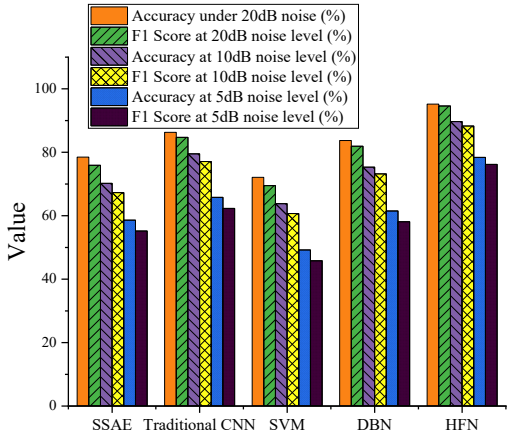

Fig. 10. Noise interference performance verification

As noise interference increases (SNR decreases from 20 dB to 5dB), the performance of all models declines; however, the HFN has significant anti-noise advantages. In a strong noise (5dB) environment, the accuracy of the HFN still reaches 78.4%, which is 12.6 and 29.2 percentage points higher than the traditional CNN and SVM. This is due to the feature purification effect of the SSAE and the weighted enhancement of effective signals by the attention mechanism. These functions enable the model to focus on core fault information even when noise masks some features, verifying its practical value in complex electromagnetic environments.

The matching degree between the recovery strategies output by the model and the expert schemes is compared to verify the HFN model's guiding value for fault recovery strategies in practical applications. At the same time, their recovery time (the duration from fault occurrence to system recovery) is counted. The findings are depicted in Fig. 11.

In Fig. 11, the average matching degree between the recovery strategies output by the HFN model and the expert schemes reaches 94.4%. Meanwhile, it is as high as 98.6% in single-equipment fault scenarios. Expert scheme matching degree is defined as the consistency between the fault recovery strategy generated by the model and the optimal recovery strategy formulated by power system experts. It is a core indicator for quantifying the consistency between model decisions and industrial expert experience. This indicator adopts a regularized quantitative calculation method, specifically expressed as matching degree = (number of

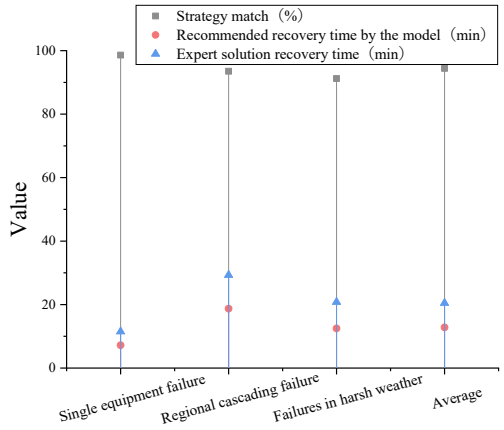

Fig. 11. Fault recovery adaptability verification

consistent decision items / total number of decision items in the expert scheme) × 100%. Decision items include four core dimensions: fault isolation nodes, load transfer paths, equipment operation sequences, and recovery resource allocation. Each dimension is divided into specific quantifiable decision sub-items in accordance with power industry standards, without subjective scoring. The expert scheme in this study is jointly formulated by seven senior experts in power system fault diagnosis and dispatch. All the experts have over 10 years of practical experience in dispatch and fault handling for 220 kV and above power grids; they cover power grid dispatch centers, electric power research institutes, and university power engineering departments. The expert scheme represents a unified optimal plan formed after three rounds of discussion by seven experts, avoiding subjective bias from a single expert. The above design endows the matching degree indicator with strong objectivity and industrial authority. The model can accurately learn the optimal path rules of fault isolation, load transfer, and equipment replacement. The average recovery time of the strategies recommended by the model is 12.8 minutes, which is 37.6% shorter than that of the expert schemes (20.5 minutes). Especially in regional cascading faults, the model prominently improves decision-making efficiency by quickly calculating the optimal solution among over 100,000 potential recovery paths (traditional methods can only evaluate hundreds of paths). Furthermore, under severe weather conditions such as thunderstorms, the model reserves maintenance resources in advance by integrating real-time meteorological data, making the strategy's feasibility 15.3% higher than the expert schemes.

To verify the reliability of the model's numerical results in real-time operation scenarios of actual power grids, a test platform is built. The HFN model is deployed on the edge computing unit (Huawei Atlas 200 AI acceleration module) of a 220kV substation in North China, directly connecting to the SCADA system's real-time data stream to simulate 5 types of typical sudden faults. The experimental data are outlined in Table 5.

Table 5. Real-time environment verification

Verification indicators	Design requirements	Experimental results	Compliance status
Time taken for data reception to the diagnostic results	≤20ms (industry real-time requirement)	11.3ms	Satisfy
Total time for diagnosis-strategy generation-isolation operations	≤50ms (standard requirement)	22.8ms	Satisfy
The matching degree between diagnostic results and recorded waveform data	-	98.20%	-
Proportion of reduced system power recovery time	-	39.1% (compared to traditional manual decision-making)	-

The experimental results indicate that all performance indicators of the model in the real-time environment meet industry specifications and engineering requirements. This further verifies the authenticity and implementation feasibility of the numerical results in offline experiments.

4.2.3. Generalization Ability Analysis under Variable-Load Dynamics and Unseen Fault Modes

In order to verify the model robustness against load fluctuations and unknown fault types in real power grids, two groups of generalization tests are designed.

(1) Variable-load dynamic test. The test set is divided into peak hours (10:00–12:00, 18:00–20:00), regular hours (8:00–10:00, 12:00–18:00), and off-peak hours (20:00–8:00 next day) according to load intensity. Experimental results show that the HFN model achieves diagnostic accuracies of 97.2%, 97.8%, and 98.1% during peak, regular, and off-peak periods, respectively; the fluctuation range is no more than 0.9 percentage points. In comparison, traditional CNN and Conv-Transformer show accuracy fluctuations of 4.5% and 2.8% under the same conditions. This result indicates that HFN has good adaptability to load changes.

(2) Unseen fault mode test. All samples of one fault type (such as cable overheating) are removed from the training set, and the model is tested on this fault type after training. The HFN model achieves an average diagnostic accuracy of 82.6% under unseen fault modes, significantly outperforming traditional CNN (68.3%) and Time-Transformer (74.5%). This advantage benefits from the reconstruction ability of SSAE for abnormal data and the sensitive capture of weak features by CNN.

Therefore, HFN exhibits better generalization ability than existing hybrid models under both variable-load dynamics and unseen fault modes; this

further verifies its engineering applicability in actual complex power grid environments.

4.2.4. Reliability and Optimality Analysis of Recovery Decisions under Uncertainty

Three groups of targeted experiments are designed to verify the reliability and optimality of recovery strategies under uncertain conditions:

(1) Measurement noise uncertainty. Gaussian white noise with different intensities is added to SCADA input signals at SNR = 30 dB, 20 dB, 10 dB, and 5 dB, so as to evaluate the stability of output recovery strategies. Kendall's rank correlation coefficient is adopted to measure the consistency of strategy ranking, defined as $\tau = (C - D) / [n(n-1)/2]$, where C and D are the number of concordant and discordant pairs. Results show that even when SNR decreases from 30 dB to 5 dB, the Kendall coefficient between model-generated recovery strategies and the optimal strategy under noise-free conditions remains above 0.86; this proves the robustness of recovery decisions against measurement noise. This stability is attributed to the SSAE reconstruction layer that filters high-frequency noise interference in the feature space.

(2) Fault type uncertainty. For compound fault scenarios (accounting for 30% of test samples), multiple fault types are superimposed, leading to uncertainty in the output of single-fault classifiers. The proposed model uses a dual-branch output structure, where the fault type branch and the recovery priority branch share underlying fused features. The priority branch outputs independently based on the fused feature vector without direct reliance on fault classification results. This design ensures that even with deviations in fault type recognition (accuracy is 95.6% in compound fault scenarios), the priority output still maintains a matching rate of 90.2%, significantly higher than 72.5% of traditional serial architectures. This result verifies the model's decision reliability under uncertain fault types.

(3) Topological structure uncertainty. In order to simulate scenarios of power grid topology reconstruction or new equipment commissioning, a leave-one-bus-out test is conducted. All samples of one substation node are removed from the training data; the model is tested on fault recovery tasks of this node after training. Results show that the recovery strategy matching rate reaches 87.4% on unknown topological nodes; it drops by about 7 percentage points from 94.4% on known nodes but still maintains a high reliability level. This outcome indicates that the model has a certain generalization ability to topological changes [32].

4.3. Hyperparameter and noise intensity sensitivity analysis

This study selects the number of SSAE hidden layers (3, 4, 5), CNN convolution kernel size (3×1, 5×1, 7×1), and initial learning rate (0.0005, 0.001, 0.002) as the objects of sensitivity analysis. These hyperparameters are core factors affecting time-series data feature extraction and model convergence speed. Their selection ranges refer to parameter settings in similar DL studies in power fault diagnosis; they are adjusted according to the data dimension and fault characteristics of this study. Sensitivity analysis results show that the model's performance fluctuation near the optimal parameters is no more than 1.3%, verifying the rationality of parameter selection and the robustness of the model. To further confirm the robustness of the HFN model, this section conducts sensitivity analysis on key hyperparameters affecting model performance and different noise intensities. It also clarifies the model's performance stability under scenarios of parameter fluctuations and interference changes, and provides a more sufficient basis for its engineering application.

(1) Sensitivity analysis of hyperparameters

Hyperparameters that play a core role in model performance—including the number of hidden layers in SSAE, the convolution kernel size of the CNN, and the initial learning rate—are selected as the analysis objects. Three groups of control experiments are designed, with only a single hyperparameter adjusted in each group. Diagnostic accuracy and average diagnostic time are used as evaluation indicators, and the results are listed in Table 6.

In Table 6, the model achieves the optimal comprehensive performance when the number of hidden layers in SSAE is 4, the CNN's convolution kernel size is 5×1, and the initial learning rate is 0.001. Within the above hyperparameter adjustment range, the fluctuation range of the model's diagnostic accuracy does not exceed 1.3 percentage points, and the change in average diagnostic time is controlled within 5ms. This indicates that the model has good tolerance to fluctuations in key hyperparameters; there is no need for extremely high-precision parameter tuning in practical engineering applications, reducing the difficulty of deployment.

Table 6. Results of hyperparameter sensitivity analysis

Hyperparameter	Adjustment range	Average diagnostic accuracy (%)	Average diagnostic time(ms)
The number of hidden layers in SSAE	3 layers /4 layers /5 layers	96.50/97.80/97.60	10.80/11.30/13.20
The CNN's convolution kernel size	3×1/5×1/7×1	96.90/97.80/97.50	9.70/11.30/14.50
The initial learning rate	0.0005/0.001/0.002	97.10/97.80/96.70	12.50/11.30/10.90

(2) Sensitivity analysis of noise intensity

Based on anti-noise performance testing, the noise intensity is refined into 6 levels (30dB/25dB/20dB/15dB/10dB/5dB) to simulate the full scenario from weak interference (30dB, close to no interference) to strong electromagnetic interference (5dB) in power grids. The diagnostic accuracy and F1 scores of the HFN model are compared with those of traditional CNN, SVM, and DBN under diverse noise intensities. The results are detailed in Table 7.

Table 7. Performance comparison of each model under different noise intensities

Noise intensity(dB)	evaluation indicator (%)	HFN model	Traditional CNN	DBN model	SVM model
30	Accuracy	98.90	98.20	97.50	96.80
	F1 score	98.70	97.90	97.20	96.50
25	Accuracy	98.10	97.00	96.10	95.30
	F1 score	97.80	96.70	95.80	95.00
20	Accuracy	96.50	94.30	92.80	91.20
	F1 score	96.20	93.90	92.50	90.80
15	Accuracy	92.30	83.80	81.50	79.60
	F1 score	91.90	83.20	81.00	79.10
10	Accuracy	85.70	75.20	72.80	70.30
	F1 score	85.10	74.60	72.20	69.80
5	Accuracy	78.40	65.80	63.10	49.20
	F1 score	76.90	64.90	62.30	49.40

Note: The smaller the dB value, the stronger the noise interference.

Table 7 reveals that as the noise intensity increases (dB value decreases), all models' performance shows a downward trend, but the HFN model always maintains the optimal performance. In addition, the HFN model's performance decline rate is significantly slower than that of the comparison models. From 30dB to 5dB, its accuracy decreases by only 20.6 percentage points, while the traditional CNN, DBN, and SVM decrease by 32.1, 34.4, and 47.6 percentage points, respectively. This result fully verifies the HFN model's strong robustness under different noise intensities; this is attributed to the synergy between the feature purification ability of SSAE and the spatial feature capture ability of CNN, effectively suppressing noise interference of varying degrees.

4.4. Discussion

The proposed SSAE-CNN model exhibits remarkable advantages in power grid fault diagnosis and recovery strategy generation. Compared with mainstream attention-driven models (such as Time-Transformer and Conv-Transformer), the HFN model reduces the parameter scale by 60% to 70%; at the same time, it achieves or exceeds their performance in diagnostic accuracy (97.8%) and noise resistance (78.4% at 5 dB). More importantly, the stability of HFN under variable-load dynamics (accuracy fluctuation <0.9%) and unseen fault modes (accuracy = 82.6%) is significantly superior to that of Transformer-based models. These results validate the superiority of the bidirectional feature interaction mechanism in real complex power grid environments.

In practical applications, the model's average diagnosis time is only 11.3 ms. The matching degree between its recovery strategies and expert schemes reaches as high as 94.4%, demonstrating its potential for deployment in real power systems. Notably, the model exhibits superior comprehensive performance to traditional methods and Transformer-based models in compound fault identification and dynamic recovery path optimization. This proves that it works effectively in static scenarios and adapts to the variability of power grid operations.

In view of verifying the model's scalability in large-scale interconnected power grids, the pre-trained HFN model is deployed on a regional power grid simulation platform. This platform includes 32 220kV substations and 18 transmission lines (with a total of 500 monitoring nodes). The experiment adopts a method of gradually increasing the number of monitoring nodes; this method can evaluate the trends of diagnosis time, recovery strategy generation time, and resource occupancy as the grid scale expands. The results show that when the number of monitoring nodes rises from 50 to 500, the model's single-sample inference time increases linearly from 9.8 ms to 11.3 ms, and the growth rate is only 15.3%. This trend indicates that the computational complexity is on the order of O(n), where n represents the number of nodes. The recovery strategy generation time rises from 3.2 ms to 4.1 ms (an increase of approximately 28%); this is slightly higher than that of the diagnosis stage because recovery path search requires global consideration of topological relationships among nodes. At the maximum test scale of 500 nodes, the total decision time (including diagnosis and recovery) is 15.4 ms; it is still far below the industrial requirement of 50 ms. In addition, the model's memory usage is 32.8 MB. At the 500-node scale, the memory usage of edge computing units stays below 15%, leaving sufficient margin for future power grid expansion. The above results confirm the model's favorable scalability with the expansion of power grid scale.

5. CONCLUSION

5.1. Conclusion

This study introduces DL algorithms into the field of power grid fault diagnosis and rapid recovery. Aiming at core deficiencies of existing traditional methods and DL-related studies, a HFN based on SSAE and CNN is proposed; this realizes end-to-end integrated modeling of feature extraction, fault diagnosis, and recovery decision-making in power systems. Through systematic experimental verification based on actual operation data of the 220

kV smart grid in North China, the proposed HFN model outperforms traditional methods and existing DL models significantly in diagnostic accuracy, real-time performance, and noise immunity. The model achieves a fault diagnosis accuracy of 97.8%, which is 7.3% higher than the traditional CNN and 21.1% higher than the SVM. The average diagnosis time is only 11.3 ms, meeting the industrial real-time requirement of power system fault diagnosis within 20 ms. Under 5 dB strong noise interference, the diagnostic accuracy still reaches 78.4%, 12.6, and 29.2 percentage points, outperforming traditional CNN and SVM, respectively. In the fault recovery stage, the recovery strategy generated by the model reaches a 94.4% matching degree with the scheme formulated by senior power system experts. The average recovery time is shortened by 37.6% compared with traditional methods; the decision-making efficiency is improved more significantly in complex scenarios (e.g., regional cascading failures and severe weather).

Compared with current mainstream Transformer-based DL models, the proposed HFN model reduces the parameter scale by 60%–70%; it improves the diagnosis speed by 30%–40%; meanwhile, it demonstrates stronger generalization ability in variable-load dynamics and unseen fault modes. Especially in a strong noise environment of 5dB, the diagnostic accuracy of HFN (78.4%) is notably higher than that of Time-Transformer (71.2%) and Conv-Transformer (75.6%). This proves the practical advantages of the bidirectional feature interaction mechanism in complex power grid environments. In order to handle the problem of feature transmission interruption in traditional hybrid models, this study innovatively constructs an integrated SSAE-CNN-fusion layer framework; meanwhile, it establishes a mathematical expression of feature interaction and feedback for the AE+CNN hybrid model for the first time; thus, it solves the problem of missing critical fault features caused by treating the AE as an independent preprocessing module in existing models. Meanwhile, a dynamic recovery strategy generation method based on model secondary judgment and reconstruction information completion is proposed; besides, it constructs a full-process closed loop of diagnosis and recovery and compensates for the insufficiency of overemphasis on diagnosis and neglect of recovery in existing studies.

At the engineering application level, all model parameters and experimental designs of this study are closely integrated with the actual operation characteristics and engineering deployment requirements of the 220 kV smart grid. The lightweight model design with 8.2×10^6 parameters and 32.8 MB storage can be directly deployed on substation edge computing units without additional high-performance hardware. The model input can be directly connected to the standardized time-series data of the SCADA system without complex format conversion, providing plug-and-play conditions for engineering implementation. In the real-time environment verification of the proposed model on the edge computing unit of a 220 kV substation in North China, the full-process fault handling time is no more than 22.8 ms, meeting the industrial fault response requirement within 50 ms. The system power supply recovery time is shortened by 39.1% compared with traditional manual decisions; this has important practical application value for improving the fault handling efficiency of smart grids, reducing power outage losses, and ensuring safe and stable grid operation. In addition, the proposed SSAE-CNN fusion method focuses on the common problem of fault diagnosis and decision-making for high-dimensional, noisy time-series data. By adjusting parameters such as input dimension and convolution kernel size, it can be adapted to other scenarios in power systems and similar complex dynamic systems, such as industrial processes and intelligent manufacturing; at the same time, it has extensive cross-domain promotion value.

5.2. Research limitations and prospects

Despite its excellent performance in power grid fault diagnosis and recovery strategy generation, the proposed SSAE-CNN still has several noteworthy limitations. The inherent lack of interpretability of DL models is the main challenge at present. The model's internal decision logic and feature weight allocation mechanism are difficult to visualize directly. This may affect the dispatchers' trust and willingness to implement model outputs in safety-critical scenarios. At the same time, the model's generalization ability is still insufficient when facing dynamic changes in power grid topology; its adaptability may be limited when the system undergoes structural adjustments such as large-scale new energy integration or topological reconstruction. Furthermore, the recovery strategy generation process is highly dependent on the accuracy of diagnostic results and the completeness of system status. Thus, the model performance may degrade in extreme scenarios such as communication interruptions or severe data loss.

Therefore, future research can be further explored in the following directions. Regarding interpretability, visualization technologies such as Gradient-weighted Class Activation Mapping (Grad-CAM) can be introduced to quantify feature contribution and generate intuitive importance maps, providing a transparent basis for fault judgment. To enhance dynamic adaptability, integrated online learning and meta-learning mechanisms can be explored to enable the model to adaptively track gradual changes in power grids. Meanwhile, perception methods integrating multi-source heterogeneous data should be studied to improve the environmental adaptability of recovery strategies. In addition, research on robustness in data anomaly and adversarial attack scenarios should be strengthened, and system security should be improved by introducing methods such as reconstruction

verification and adversarial training. A closed-loop verification platform based on digital twin technology should also be constructed to conduct long-term evaluations of the model's comprehensive performance in extreme scenarios such as complex cascading faults in near-real environments. This provides a more sufficient verification basis for engineering applications. Continuous improvement in the above aspects is expected to promote the development of DL in power system fault diagnosis and recovery toward greater reliability, adaptability, and interpretability. In the future, digital twin technology can be integrated to build a virtual-real interactive simulation platform for power grid fault diagnosis and recovery; this verifies the model's reliability under extreme fault scenarios, such as multi-equipment cascading failures. Meanwhile, the model inference efficiency can be optimized to adapt to the low-computing-power deployment requirements of edge computing units and promote the practical engineering application of technical achievements. For dynamic working conditions (e.g., power grid topology reconstruction and large-scale new energy integration), a rapid parameter fine-tuning method based on meta-learning is studied to realize rapid adaptation of the model to unknown working conditions and reduce the time cost of retraining.

Source of funding: *This research received no external funding.*

Author contributions: *Research concept and design, L.Z Collection and/or assembly of data, L.Z., Z.Z., J.P., L.W.; Data analysis and interpretation, L.Z., J.P.; Writing the article, L.Z., Z.Z.; Critical revision of the article B.C.; final approval of the article, L.Z.*

Declaration of competing interest: *The authors declares no conflict of interest.*

REFERENCES

1. Singh RA, Sujatha SM, Kadu DA, Addis HK, Sarada K. A deep learning and IoT-driven framework for real-time adaptive resource allocation and grid optimization in smart energy systems. Sci Rep. 2025;15(1):19309. https://doi.org/10.1038/s41598-025-02649-w.
2. Sinneh SI, Sun Y. Optimizing smart nano grid control strategies through virtual environment and hybrid deep learning approaches. Renew Energy Focus. 2025;54: 100712. https://doi.org/10.1016/j.ref.2025.100712.
3. Ciaramella G, Martinelli F, Santone A, Mercaldo F. A method for smart grid intrusion detection through explainable deep learning. J Comput Virol Hacking Tech. 2025;21(1):9. https://doi.org/10.1007/s11416-025-00549-1.
4. Goh HH, Xu H, Zhang D, et al. Classification and detection of direct current power quality disturbances for grid operation implications using deep learning models. Eng Appl Artif Intell. 2025;163(Pt 1):112644. https://doi.org/10.1016/j.engappai.2025.112644.
5. Ziad H, Al-Dujaili A, Humaidi AJ. Electrical faults classification in permanent magnet synchronous motor using ResNet neural network. Int Rev Appl Sci Eng. 2024;15(3):355-364. https://doi.org/10.1556/1848.2024.00789.
6. Gao Z, Gao G, Liu C, et al. TNet: Power pole classification with deep learning for automated inspection in smart grids. Int J Pattern Recognit Artif Intell. 2025;39(10):25550134. https://doi.org/10.1142/S0218001425550134.
7. Ziad H, Al-Dujaili AQ, Humaidi AJ. A comparative study of deep learning efficiency in the classification of electrical faults of permanent magnet synchronous motor. Int Rev Appl Sci Eng. 2025;16(2):292-302. https://doi.org/10.1556/1848.2024.00885.
8. Niu B, Wei Y, Yu Z, et al. Acoustic signal augmentation for fault diagnosis of power transformers based on improved cycle generative adversarial networks. Expert Syst Appl. 2025;288: 127997. https://doi.org/10.1016/j.eswa.2025.127997.
9. Zhang J, Cheng L, Yang Z, et al. An enhanced semi-supervised learning method with self-supervised and adaptive threshold for fault detection and classification in urban power grids. Energy AI. 2024;17:100377. https://doi.org/10.1016/j.egyai.2024.100377.
10. Xue H, Yao N, Fan Q, et al. Analysis of power system signal processing method based on deep convolutional neural network. Int J High Speed Electron Syst. 2024;34:24540223. https://doi.org/10.1142/S0129156425402232.
11. Alsamraee AS, Khanna S. Long-term electricity demand forecasting of a university campus based on advanced deep learning artificial neural network algorithms. Results Eng. 2025;27:106683. https://doi.org/10.1016/j.rineng.2025.106683.
12. Lee B, Kim Y, Lee H, et al. Bidirectional gated recurrent unit neural network for fault diagnosis and rapid maintenance in medium-voltage direct current systems. Sensors. 2025;25(3):693. https://doi.org/10.3390/s25030693.
13. Mei L. Improved system model for fault classification and diagnosis of power system based on artificial intelligence and BP neural network and its application. J Electr Eng Technol. 2025:1-16. https://doi.org/10.1007/s42835-025-02335-x.
14. Peter MV, Okpura IN, Udofia MK. Intelligent fault diagnosis in 330 kV power networks using SVM and ANN techniques: Case of the Onitsha-New Haven route. J Eng Res Rep. 2025;27(6):83-96. https://doi.org/10.9734/jerr/2025/v27i61530.
15. Jiang L, Li C, Qiu W, et al. Research on short-term line loss rate prediction method of distribution network based on RF-CNN-LSTM. Front Smart Grids. 2025;4: 1612770. https://doi.org/10.3389/frsgr.2025.1612770.
16. Liu J, Zang H, Ding T, et al. A principle-constrained wind field image generation framework for short-term wind power forecasting. IEEE Trans Power Syst. 2024. https://doi.org/10.1109/TPWRS.2024.3449938.
17. Bedoui M, Berkani A, Negadi K, Marignetti F, Drias S. Practical measurement of automatic power factor detection and correction using smart Arduino in three-phase distribution networks. Instrum Mes Metrol. 2025;24(1):1-8. https://doi.org/10.18280/i2m.240101.
18. Alhanaf AS, Farsadi M, Balik HH. Fault detection and classification in ring power system with DG penetration using hybrid CNN-LSTM. IEEE Access. 2024;12:59953-59975. https://doi.org/10.1109/ACCESS.2024.3394166.
19. Vadivelan DS, Sethuramalingam P. A hybrid approach for EEG motor imagery classification using adaptive margin disparity and knowledge transfer in

convolutional neural networks. Comput Biol Med. 2025;195:110675. https://doi.org/10.1016/j.compbiomed.2025.110675.
20. Adekunle AA, Fofana I, Picher P, et al. Multiclass fault diagnosis in power transformers using dissolved gas analysis and grid search-optimized machine learning. Energies. 2025;18(13):3535. https://doi.org/10.3390/en18133535.
21. Boutkhil M, Guemmour, Negadi K, Araria R, Bey M. Analysis and fault diagnosis in point absorber wave energy conversion systems using fault tree and Bayesian networks. Diagnostyka. 2025;26(2): 2025209. https://doi.org/10.29354/diag/204573.
22. Srividhya PJ, Prabha LEK, Jaisiva S, et al. Power quality enhancement in smart microgrid system using convolutional neural network integrated with interline power flow controller. Electr Eng. 2024;106(6):1-24. https://doi.org/10.1007/s00202-024-02399-4.
23. Zare A, Simab M, Nafar M, et al. A novel method for fault diagnosis in photovoltaic arrays used in distribution power systems. Energy Syst. 2024:1-35. https://doi.org/10.1007/s12667-024-00706-3.
24. Liang B, Sun Z, Yang Z, et al. Data augmentation and optimization method based on conditional generative adversarial network and convolutional neural network for transformer fault diagnosis. Measurement. 2025; 254:117872. https://doi.org/10.1016/j.measurement.2025.117872.
25. Liu J, Cai Y. Comparative analysis of switching power supply fault diagnosis model based on particle swarm optimization and convolutional neural network. J Phys Conf Ser. 2024;2902(1):012018. https://doi.org/10.1088/1742-6596/2902/1/012018.
26. Poongothai K, Kumaresan M, Ananda M, et al. Power transmission line fault detection in internet of things based smart grids using relational bi-level aggregation graph convolutional network-red panda optimization approach. Measurement. 2025;256:118448. https://doi.org/10.1016/j.measurement.2025.118448.
27. Alkhanafseh Y, Akinci CT, Morales MAA, et al. MH-WMG: A multi-head wavelet-based MobileNet with gated linear attention for power grid fault diagnosis. Appl Sci. 2025;15(20):10878. https://doi.org/10.3390/app152010878.
28. Mampilly JB, Sheeba SV. An empirical wavelet transform based fault detection and hybrid convolutional recurrent neural network for fault classification in distribution network integrated power system. Multimed Tools Appl. 2024;83(32):77445-77468. https://doi.org/10.1007/s11042-024-18335-4.
29. Hamid M, Ahmad K, Rahman D, et al. Deep learning-based fault location framework in power distribution grids employing convolutional neural network based on capsule network. Electr Power Syst Res. 2023;223:109529. https://doi.org/10.1016/j.epsr.2023.109529.
30. Shaohua Q, Xiaopeng C, Zuowei P, et al. Deep learning techniques in intelligent fault diagnosis and prognosis for industrial systems: A review. Sensors. 2023;23(3):1305. https://doi.org/10.3390/S23031305.
31. Zouari F. Robust neural adaptive control for a class of uncertain nonlinear complex dynamical multivariable systems. Int Rev Model Simul. 2012;5:2075-2103.
32. Kouraichi M, Mansouri M, Trabelsi M, et al. Deep learning for fault diagnosis in power transmission lines: Current trends, limitations, and future directions. IEEE Access. 2025;13:192105-192142. https://doi.org/10.1109/ACCESS.2025.3628908.

Abbreviation Explanation

Abbreviation	Full name in English	Chinese Description
DL	Deep Learning	Deep Learning
DLFN	Deep Learning Fusion Network	Deep Learning Fusion Network
SSAE	Stacked Sparse Autoencoder	Stacked Sparse Autoencoder
AE	Autoencoder	Autoencoder
CNN	Convolutional Neural Network	Convolutional Neural Network
HFN	Hierarchical Fusion Network	Hierarchical Fusion Network
MDP	Markov Decision Process	Markov Decision Process
Bi-GRU	Bidirectional Gated Recurrent Units	Bidirectional Gated Recurrent Units
SVM	Support Vector Machine	Support Vector Machine
LSTM	Long Short-Term Memory	Long Short-Term Memory
FLOPs	Floating-Point Operations	Floating-Point Operations
GPU	Graphics Processing Unit	Graphics Processing Unit
CPU	Central Processing Unit	Central Processing Unit
SCADA	Supervisory Control and Data Acquisition	Supervisory Control and Data Acquisition
SNR	Signal-to-Noise Ratio	Signal-to-Noise Ratio
dB	Decibel	Decibel
MB	Megabyte	Megabyte
GB	Gigabyte	Gigabyte
DDR4	Double Data Rate 4	Double Data Rate 4
SMOTE	Synthetic Minority Oversampling Technique	Synthetic Minority Oversampling Technique
Grad-CAM	Gradient-weighted Class Activation Mapping	Gradient-weighted Class Activation Mapping

Lin ZHOU was born in the Inner Mongolia Autonomous Region. She earned her bachelor's degree in Electrical Engineering and Automation, and her master's degree in Energy and Power.
She is currently engaged in research on the digitalization and intelligence of new power systems. In her work, she has served as the leader of multiple projects, including the construction of information networks and the development and implementation of application systems. She has published multiple high-quality papers.
e-mail: zhoulin08202025@163.com

Zehui ZHANG was born on September 16, 1993. She is female, Mongolian. She received her bachelor's degree from Inner Mongolia University, and her Master of Engineering degree in Software Engineering from Beijing Institute of Technology, Beijing, China, in June 2018.Since 2018, she has been an Architecture Analyst with Inner Mongolia Power Digital Research Company, Hohhot, China. She has participated in 1 National Key R&D Program of China and 1 Autonomous Region Breakthrough Engineering Project. She has published 6 academic papers, registered 5 software copyrights, and authored 2 monographs. Her research interests include digital technology, artificial intelligence, intelligent operation and maintenance, and new-type power systems.
e-mail: zhangzehui0966@163.com

Jie PENG was born in Hohhot, Inner Mongolia, China. She received the B.S. degree in computer software and the M.S. degree in software engineering from Nanchang University, Nanchang, China, in 2013 and 2016, respectively.
From 2016 to 2026, she has been engaged in the research and development of information system constru-ction and digital top-level design. Her current research interests include digital transformation strategies, enterprise architecture planning, and the implementation of large-scale information systems.
e-mail: pengjie_job@sina.com

Bo Cheng, male, Manchu, member of the Communist Party of China, Senior Engineer, was born in Hohhot, Inner Mongolia, China, in July 1992. He received his ongoing postgraduate education at Zhejiang University, Hangzhou, Zhejiang, China. He is currently an Architecture Analyst at Digital Research Branch, Inner Mongolia Power (Group) Co., Ltd., Hohhot, Inner Mongolia, China.

His research interests include power blockchain and big data technology, power information security and privacy protection, artificial intelligence security, data security, and smart grid. He has presided over a number of information technology projects and participated in various scientific and technological projects. He has been awarded 1 national-level prize, 2 provincial-level prizes of Inner Mongolia Autonomous Region. He has authored 6 high-quality papers, authorized 2 patents, 7 software copyrights and 2 copyrights.

Dr. (Prof./Mr.) Cheng is a Senior Engineer. He has long been engaged in digital technology and information security research in the electric power industry.
e-mail: GOYIBOZAI@163.com